

Introduction

The Morgan Bridge is currently one of the few remaining covered wooden bridges making use of the queenpost truss form. This report investigates the engineering aspects of queenpost bridges in general, and the Morgan Bridge in particular, including the effect of modifications made to the structure in 1979. It will also compare the use of experimental load testing with the more common practice of computational modeling as a means of analyzing the structural behavior of a unique, timber bridge.

Historical Perspective

The history of structural engineering is not only an interesting topic to engineers, it is also essential for a complete understanding of structures. Engineers must understand the reliability of materials, design details, and construction techniques used in the past so that they can make appropriate, informed decisions about ageing structures in the future. Ever changing building codes, methods of construction, and material strengths add difficulty and confusion to projects involving structures that were built generations ago. The ability to make accurate assessments of the condition of existing structures may help prevent unnecessary replacements, and also assist engineers to make appropriate decisions about rehabilitation. To fully appreciate and therefore fully understand any structure, engineers must be able to identify not only its structural behavior, but also its place in society, both socially and symbolically.

There are 101 known queenpost covered wooden bridges left today, which account for a little over 10 percent of all remaining covered bridges in the United States.¹ Similar, but generally shorter, kingpost bridges account for a little over 3 percent. These are fairly low numbers, considering the relative ease with which both types could be constructed, and the consequently large number that were likely once in use. It is not surprising, however, that the simplest bridges were not among the first to be protected, as they were short spans that broke no new technical ground, and typically treasured only locally.

Nevertheless, this study of the most basic truss forms should prove valuable, since they established many of the principles that made the more-complex designs possible. These two forms date back to at least the sixteenth century. The kingpost is unarguably the simpler form of the two, consisting of a bottom chord, a center vertical member (the kingpost) and two diagonal bracing members that extend from the top of the kingpost to the ends of the bottom chord. The bottom chord and kingpost act in tension, and the diagonal braces are in compression under typical loading conditions. The forces in the structural members are illustrated in Figure 1, where compression members are labeled “C,” and tension members are labeled “T.”

¹ *World Guide to Covered Wooden Bridges*, 1989.

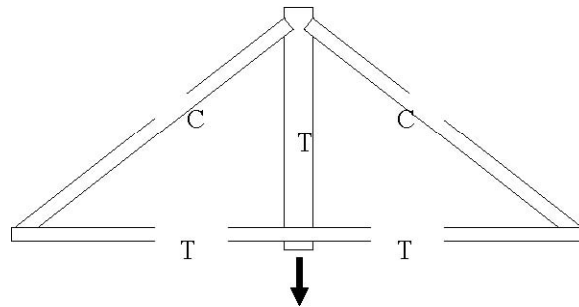


Figure 1. Typical kingpost configuration

The queenpost is a variation of the kingpost form that was most likely developed to span longer distances. The queenpost form contains three panels, separated by two vertical tension members (queenposts). As in the kingpost, the bottom chord is under tension and the diagonals are in compression, as shown in Figure 2. The center panel, between the two queenposts, is an open box formed with the top and bottom chords. Having no diagonal braces, it would be unstable, except that the truss must have an effectively continuous bottom chord capable of resisting moment loads at the bottom of the queenposts.

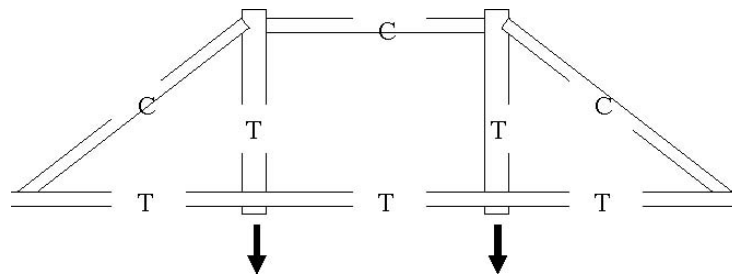


Figure 2. Typical queenpost configuration

The Morgan Bridge

An inspection of the Morgan Bridge made it clear that, while its design was carefully planned, its purpose was purely utilitarian. Many of the timber members exhibited unused notches, indicating that the bridge may have been built of reclaimed timbers. As detailed in the HAER historical report, records clearly indicate the rebuilding of the bridge during 1898-99, but the original bridge may well have been constructed at this location as early as 1886. Its design may have differed from the 1899 form, and original timbers could have been reused, leaving the notches as remnants from its original construction.

When the Morgan Bridge was rebuilt in 1899, it most likely resembled the structure illustrated in Figure 3. In typical queenpost form, there were no members in the middle panel, but both diagonal braces and counterbraces in the side panels. Only three floor beams were used to transfer loads from the deck to the truss. Metal rods in the side panels doubled as tension members (posts) in the truss and as a means to transfer load from the floor beams. Since the bridge had no post at its center, short rods were used to connect the floor beam to the lower chords at mid-span. For reasons lost to time, an odd post was inserted in the north side panel, but not quite at the intersection of the two diagonal members. The south side panel had no counterpart.

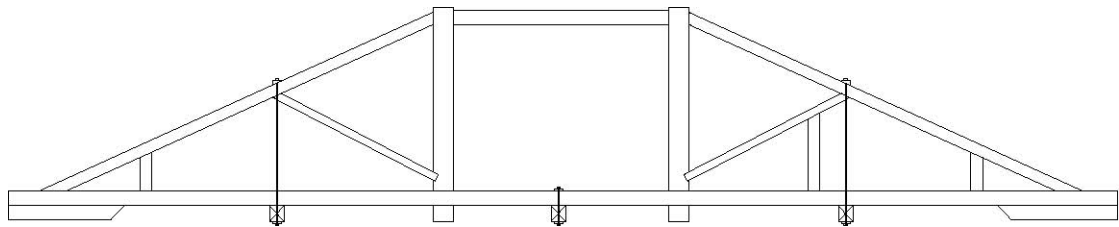


Figure 3. 1899 Configuration of the Morgan Bridge

In 1979, the Vermont Agency of Transportation rehabilitated the Morgan Bridge to the configuration illustrated in Figure 4. Four floor beams were added to bring the total to seven, and as in the original construction, metal rods were used to attach the new floor beams to the truss. It appears that the engineers' primary concern at the time was the floor, rather than the truss itself. Except for the addition of diagonals in the center panel to create a new panel point for the center floor beam support rod, there is no indication that individual truss members were strengthened. One area of particular interest is whether these new diagonals significantly altered the truss's performance.

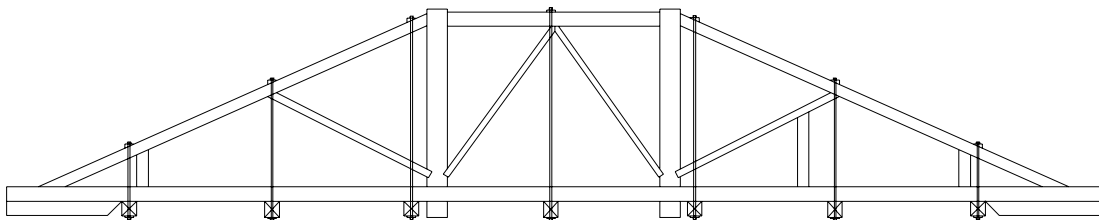


Figure 4. Current (post-1979) Configuration of Morgan Bridge

The 1979 rehabilitation opened up another interesting area for exploration as well. Comparing experimental load tests with computer models of the current configuration should provide evidence and feedback to determine if the selected models can be used to evaluate other configurations of timber bridges—in this case, the 1899 design—with confidence, and to understand the limits of the models. Since rehabilitation is often

necessary if these structures are to remain in service, assessing the positive and negative impacts of alterations can help engineers and owners to make better decisions when questions arise about the condition of other existing bridges.

EXPERIMENTAL LOAD TESTING OF THE MORGAN BRIDGE

Testing Procedure

The vehicle used to load test the Morgan Bridge was a Chevrolet Astro Van. Figure 5 is a photograph of the vehicle and Figure 6 illustrates the assumed axle weights, based on the curb weight data obtained from the manufacturer's specifications.



Figure 5. Chevrolet Astro van used in experimental load testing

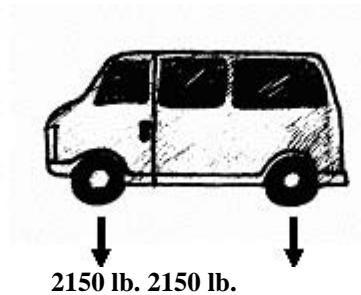


Figure 6. Assumed axle weights of load test vehicle

Instrumentation used to measure the bridge's response to live loading was placed on the bridge prior to testing. The truck was driven across the bridge from north to south several times, stopping at predetermined locations along the span so that data could be recorded from the instrumentation. These selected stopping points were chosen based on preliminary computer modeling done prior to field work. Tape was used to mark the exact axle locations during the first run of the truck across the bridge so that the same

locations could accurately be found in each subsequent run. The arrows in Figure 7 indicate the locations at which data were recorded.

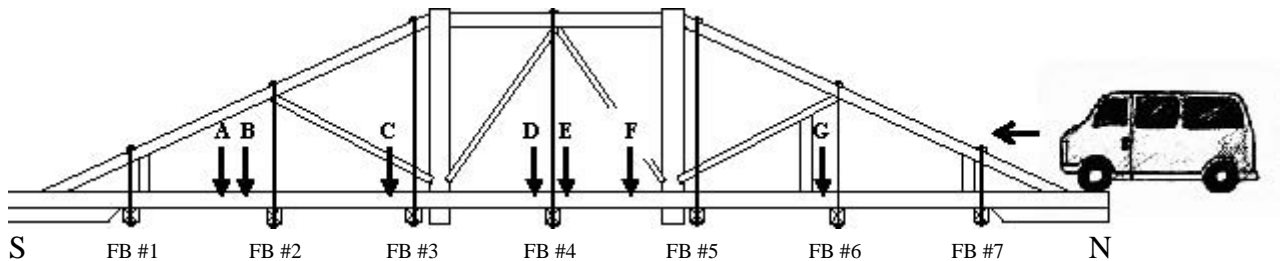


Figure 7. Typical front axle locations along the west truss (view from inside bridge)

Instrumentation

Field testing of the Morgan Bridge involved the measurement of displacements, or structural movement under load, and strains in selected members. Several types of instrumentation were employed to acquire this data, including:

- Linear Variable Differential Transformer (LVDT)
- Position Transducers
- Extensometer
- Strain Gages
- Surveying Equipment

An LVDT may be used to measure the relative movement between any two points. Using an LVDT alone is somewhat limiting in fieldwork, so a linear spring-cable system was introduced to the assembly. The cable allowed measurements between two points spaced far apart, and the spring allowed the LVDT to capture both positive and negative movements. The LVDT assembly shown in Figure 8 had one end attached to the bridge at mid-span and other end fixed to a point in the stream bottom.



Figure 8. Linear variable differential transformer (LVDT) assembly

Two Position Transducers were used in the load-testing program. Their assembly also employed a linear spring-cable assembly similar to that used with the LVDT, as shown in Figure 9. The difference in the two assemblies is that the position transducers capture relative movement through a different mechanism than the LVDT. Additionally, the position transducer's range of motion is only 4 centimeters, as opposed to 6 centimeters for the LVDT used. In Figure 9, the position transducer is mounted underneath the top chord of the west truss, adjacent to the north queenpost, and the cable runs diagonally to a position on the east truss, adjacent to the south queenpost. This was done to examine out-of-plane effects of live loading on the bridge.



Figure 9. Position transducer assembly

An extensometer also measures the relative movement between two points. It is a small instrument with only a ¼-inch range of motion, but it is highly accurate and a good instrument for measuring movements across connections. For these tests, an extensometer was mounted at the connection between one of the new diagonal members in the center panel and a queenpost, as shown in Figure 10.

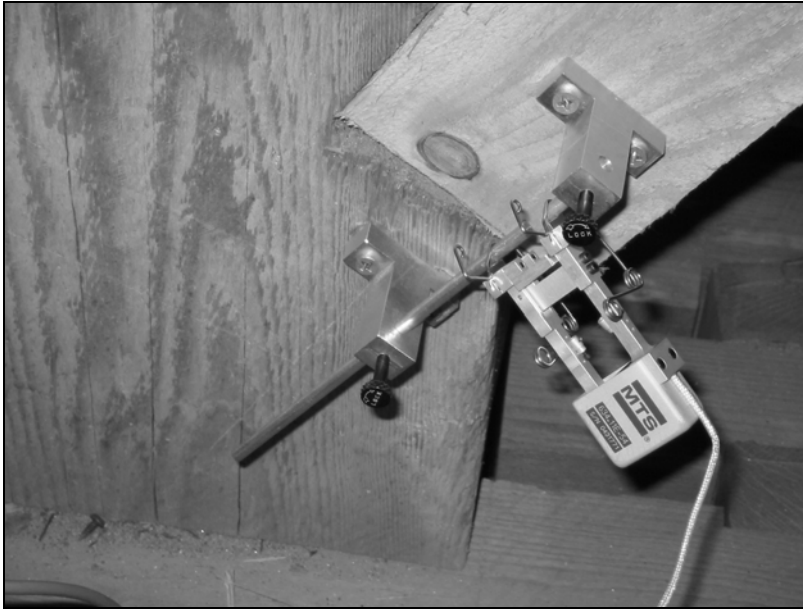


Figure 10. Extensometer spanning the joint between a diagonal and queen post

Strain gages were used to measure the axial strain in bridge members when subjected to live loading. While it is possible to mount them to wood members, they are more accurate when mounted to metal. Figure 11 shows one of the strain gages mounted to a metal rod. The gages used were capable of capturing up to 5 percent strain.



Figure 11. Strain gage mounted to a metal rod on the west truss

Surveying equipment, normally used for land surveying, was used to collect overall deflection data. The equipment included a total station and several reflective prism targets. These are shown in Figures 12 and 13, respectively. Prisms were securely attached to the structure using custom-built brackets, and their initial positions were measured and recorded by the total station. These positions corresponded to the bridge in its dead load condition. The positions of these prisms were again measured and recorded by the total station under the various live load conditions to allow calculation of the deflection at each target location.



Figure 12. View of total station with respect to the bridge



Figure 13. Typical reflective prism target and bracket

STATIC ANALYSIS OF THE MORGAN BRIDGE

Geometry and model construction

Based on information collected in the field, a computer model of the Morgan Bridge truss was developed using the MASTAN2 structural analysis software.² A three-dimensional model will be presented briefly later in the report, but a majority of the analysis, both in the field and using the model, was performed in two dimensions, and on the west truss alone. Since the two trusses appeared to be alike, it was believed that they would perform the same way.

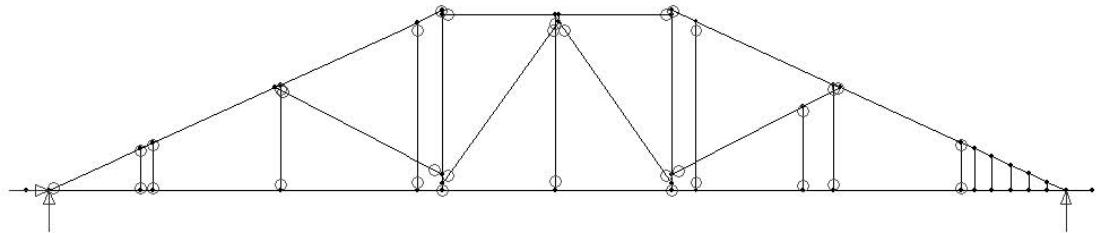


Figure 14. Single-line diagram of west truss model

As the diagram in Figure 14 shows, the model of the bridge used had forty-six

² MASTAN2, version 2.0, developed by R. D. Ziemian and W. McGuire, 2000.

nodes connecting sixty-six beam elements. The elements represent the centerlines of the actual member dimensions, as measured in the field. While a typical truss model assumes pinned connections at all nodes, in this case only the ends of certain members are pinned, while others are modeled as fixed connections. A fixed connection allows the transfer of moment between members, but a pinned connection is capable of transferring only axial forces. The circles shown in the model indicate the connections modeled as pins. (The actual bridge has fixed connections wherever a member, such as the top or bottom chord, is continuous across a connection, but there is limited rotational flexibility between the chords and the posts, so pin connections were used.) One location where all members were modeled as fixed was at the north (right) end of the west truss, where a triangular metal plate is securely fastened between the bottom chord and top diagonal bracing. The plate was modeled as a series of vertical steel elements, fixed at the top and bottom where they connected to the timber truss members. This plate can be seen in the Figure 15 below.



Figure 15. Triangular metal plate in northwest corner of west truss

In addition to capturing the varying joint stiffnesses between members, an attempt was also made to capture any significant eccentricities that might affect the structural behavior of the bridge. One of these eccentricities was at the connection between the new (1979) bracing in the center panel and the original top chord. The eccentricity of this connection can be seen in Figures 4, 14, and 16.



Figure 16. Eccentricity of connection at mid-span of top chord.

Another variable thought to influence the bridge was the composition of the bottom chord. Since the bridge is approximately 60' long, the builders used three parallel pieces of wood, staggered and spliced along their lengths, to act as one continuous piece with a varying cross section. The full cross section showing all three pieces is shown in Figure 17, and Figure 18 is a plan view that shows the scarf joints and member end locations. The highlighted areas along the chord illustrate individual members that were included in the model. The basis for this selection is the conservative assumption that anywhere an individual member terminates, whether at a butt joint or scarf joint, it is not likely to contribute significantly to the overall strength of the chord.

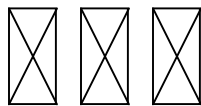


Figure 17. Cross section of lower chord



Figure 18. Plan view of lower chord with contributing members highlighted

The external boundary conditions at the ends of the bridge were modeled as simple supports, with the exact point of support located at the intersection of the bottom chord and queenpost brace centerlines. If it is assumed that the reaction force from the

abutment beam seat is distributed evenly over the portion of the bolster beam supported by the abutment, then the resultant of the distributed reaction may be assumed to act at the midpoint of this supported length.

Mechanical Properties of Structural Members

One of the most challenging aspects of modeling the structural behavior of a nineteenth-century timber bridge is determining how best to quantify the mechanical properties of its members, especially its wooden members. Experimental means exist for determining certain mechanical properties, but they are expensive and, consequently, unavailable in most instances. The only definitive information regarding the species of wood used in the Morgan Bridge came from the U. S. Forest Products Laboratory, which tested a small piece of wood from one queenpost and determined that it was spruce.

The laboratory can usually identify the genus of a sample through microscopic examination and its knowledge of the anatomical characteristics of different woods. So, while the exact species of spruce could not be provided, it was assumed for the purposes of this analysis that it is eastern spruce, the only species that would have been readily available in New England. For such a small bridge, it is unlikely that wood would have been shipped from the southern states, or the Rockies, where other varieties of spruce are prevalent. Table 1 lists the mechanical properties assumed for the timber members in Morgan Bridge, as well as the mechanical properties assumed for the metal rods.

Table 1. Mechanical Properties used in Computer Model

Element	Material	E (psi)	v	Density (pcf)
Wood members	Eastern spruce	1,400,000	0.4	27.9
Metal rods	Mild steel	29,000,000	0.3	490

Panel Point Loads due to Live Loads

MASTAN2 computes dead loads internally using user inputs for cross-sectional area and material density. For vehicular live loads, it was desired to apply the wheel loads to the computer model in such a way that appropriate comparisons could be made between the model results and the field data. Using known axle weights and distances, it was possible to determine the distribution of loads from the tires to the deck, thence to the stringers, floor beams, and, finally, the truss. It was assumed for these calculations that the stringers were simply supported between the floor beams, and that the floor beams were simply supported between the east and west trusses. Table 2 summarizes the panel-point

loads resulting from the truck located at the positions shown in Figure 7.

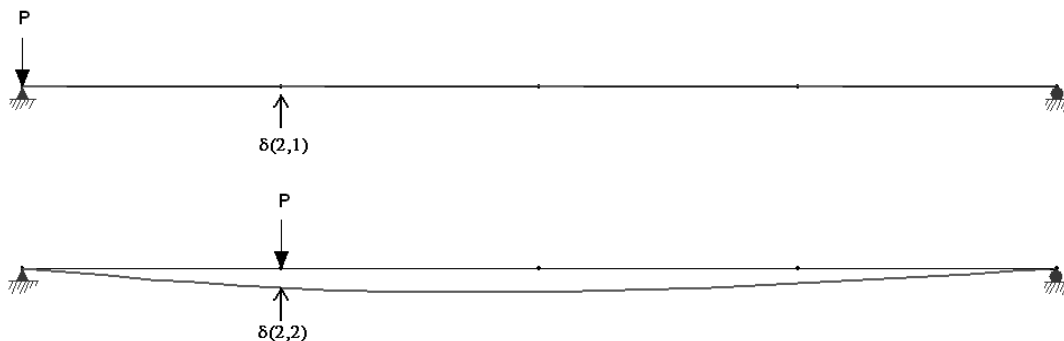
Table 2. Panel Point Loads Resulting from Live Load Positions

Floor Beam	Front Axle Location Reaction						
	A	B	C	D	E	F	
FB No. 1	586	420					
FB No. 2	903	901					
FB No. 3	659	827	1075	142			
FB No. 4			894	932	993	554	
FB No. 5			180	1075	924	1206	155
FB No. 6					232	389	919
FB No. 7							1075

Influence Lines

Engineers often use graphical methods to describe the behavior of a structure. Common methods include shear, moment, and axial force diagrams, which are often used to demonstrate the effect of fixed or dead loads. Bridge live-load analysis requires the use of another graphical method due to the moving live loads. The curves generated are called an influence lines. Influence lines differ from the other diagrams in that they represent the effect of a moving load at one particular location on the bridge, rather than the effect of all loads at all locations on the bridge. Since the field test data on the Morgan Bridge were taken at specific points while the vehicle was moved to several different locations, influence lines provide a useful way to present and compare test data and computed values.

Figures 19 and 20 form an elementary example showing the influence line of quarter-point deflection on a simply supported span.



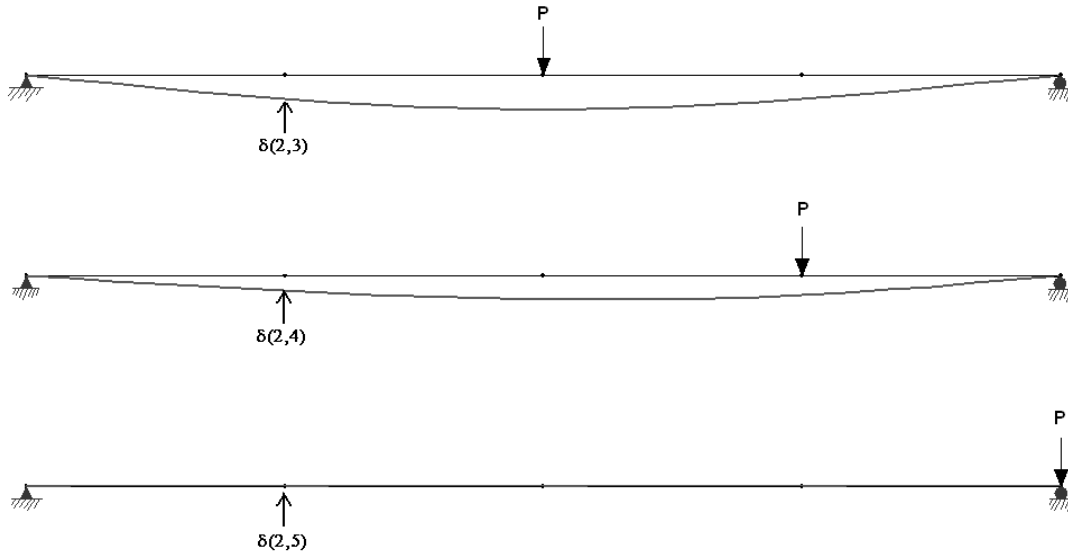


Figure 19. Series of loading conditions on one beam used to develop an influence line

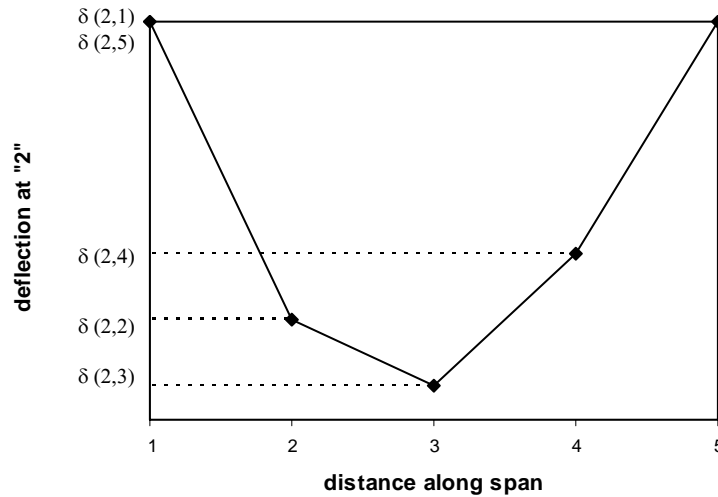


Figure 20. Influence line for quarter point deflection of a beam with simple supports

TRUSS BEHAVIOR UNDER DEAD LOAD

The dead load of each structural member was computed using member sizes obtained from field measurements and the weight densities given in Table 1. The dead load is the sum of the weights of all truss members plus the weights of all floor and roof components. The existing floor system was well documented so its weight could be computed and applied to the appropriate panel points. With the exception of fewer floor

beams and panel points, it was assumed that the original floor system was similar to the existing one. Detailed measurements were not made of the roof, but it is most likely similar to the original structure, so a weight comparable to the floor system was used and applied to the top chord where it connects to the roof truss. The only dead load neglected in the analysis was that of the siding.

Figures 21 and 22 show the axial force diagrams for the existing and original configurations, respectively. The thickness of each member in these diagrams is indicative of its stress, with the shaded members in compression and the unshaded ones in tension. While the diagrams are not labeled for simplicity, they are drawn to the same scale. The compression forces in the top chord and tension forces in the bottom chord are similar for both configurations. Specifically, the maximum compression in the top chord is approximately 15,200 pounds for the existing configuration (Figure 21) and 12,500 pounds for the original configuration (Figure 22). The maximum tension in the bottom chord is 14,000 pounds for the existing configuration and 11,300 pounds for the original configuration. The forces due to dead loads in the existing configuration are approximately 20 percent higher than those in the original configuration, which is due to the addition of four floor beams in 1979, as well as the significant change in the floor system load distribution that resulted from this change. Prior to the rehabilitation, the bolster beams likely distributed more load from the floor system to the abutments, but with addition of floor beams so close to the bolster beams, their role has likely been reduced significantly. The forces in both configurations are typical for the queenpost form, with only the bottom chord and queenposts in tension (plus the floor beam hanger rods in the existing configuration).

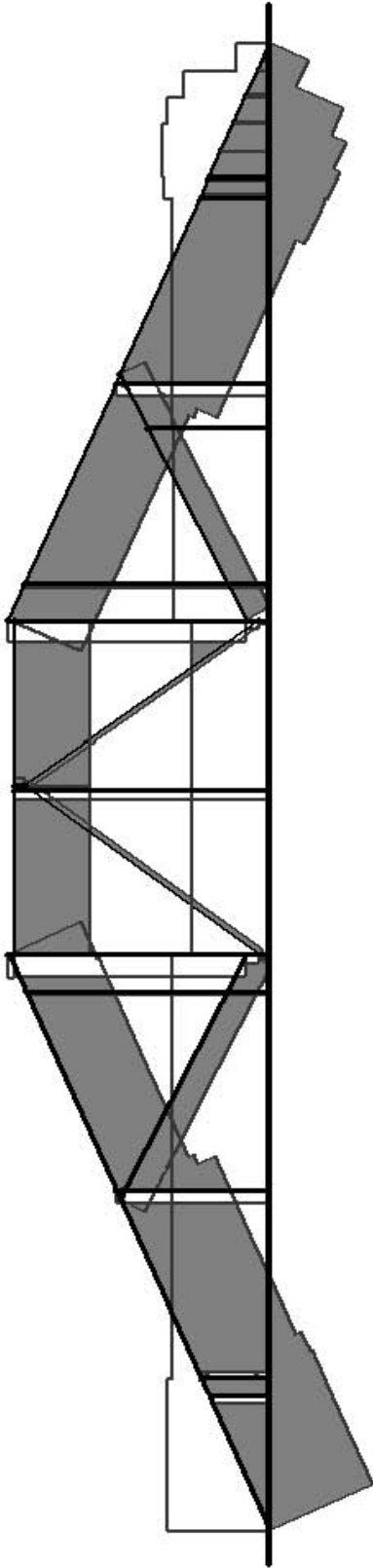


Figure 22. Axial Forces Caused by Dead Loads in Existing Configuration

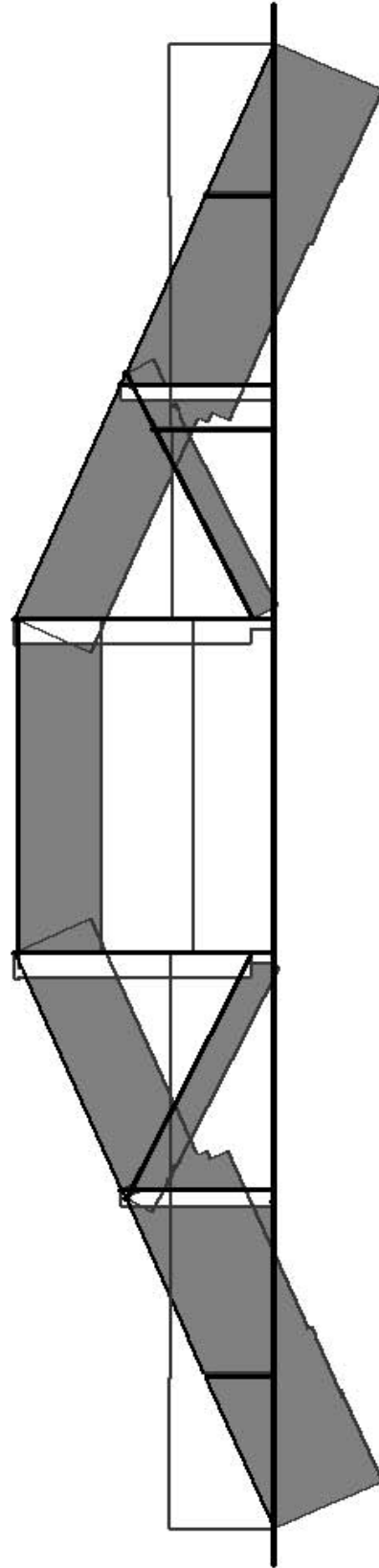


Figure 23. Axial Forces Caused by Dead Loads in Original Configuration

TRUSS BEHAVIOR UNDER LIVE LOAD

Mid-Span Deflection and Overall Bridge Stiffness

Due to the considerable variability in geometry and materials, it is difficult to draw comparisons among different covered wooden bridges. Stiffness can be a convenient, normalizing tool with which to make this comparison, as it reflects the behavior of the bridge system, rather than that of individual members. The formula for stiffness is:

$$k = \frac{F}{\delta}$$

where: k = flexural stiffness of the system
 F = force applied to the system
 δ = overall displacement of the system

In the field, an LVDT was used to take mid-span deflection measurements of the bridge under vehicular live loading. Figure 23 shows two photographs of this test assembly. On the left is the position of the LVDT at mid-span, as seen from inside the bridge. It was firmly connected to the lower chord, near the center vertical rod. The cable ran down through a space between the chord and deck, and was securely fastened to a tripod that sat in the water, held down by rocks and laboratory weights. An initial displacement was induced into the assembly by stretching the spring, to allow for both positive and negative deflections under live load. The cable in Figure 23 is darkened for clarity.

Eleven trials were performed with this instrumentation in place. Figure 24 shows the results of the mid-span deflection tests. The independent (horizontal) axis demonstrates the location of the vehicle's center of gravity along the west truss, with zero at the south end, and the dependent (vertical) axis is the mid-span bridge deflection measured by the LVDT. A negative deflection value indicates that the bridge was moving downward. The dashed line shown on the plot is an interpolation of the likely influence line for mid-span deflection.

Mid-span deflections obtained from the computer model are provided in Table 3, along with the mean and standard deviation of the experimental data plotted in Figure 24.



Figure 23. Measuring mid-span bridge deflections with LVDT

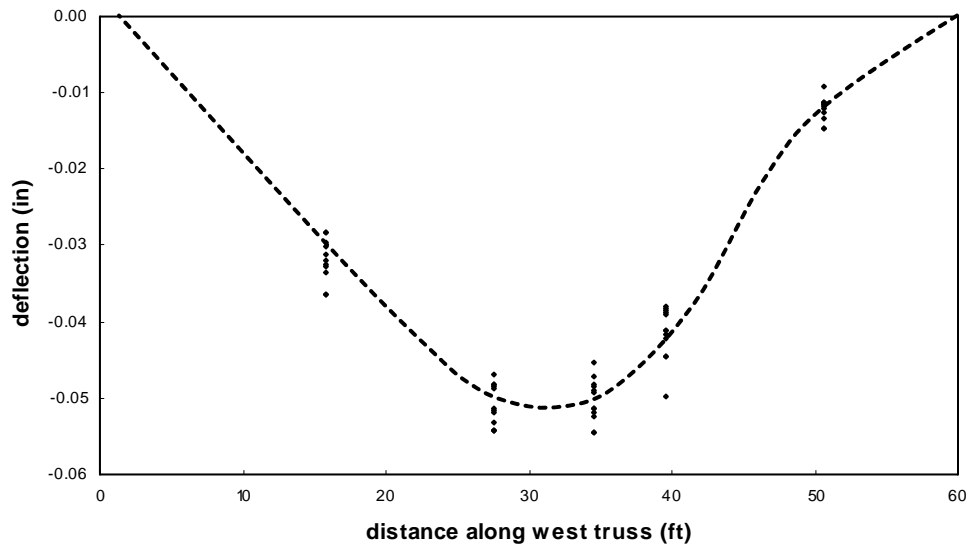


Figure 24. Influence line for mid-span deflection as a result of live load

Table 3. Comparison of mid-span deflection data

Truck Position		Field Data		Computer Model
Description	Location (ft.)	μ_{δ} (in.)	σ_{δ} (in.)	δ (in.)
A	11.05	-0.0315	0.0025	-0.0360
C	22.80	-0.0506	0.0026	-0.0523
D	29.80	-0.0499	0.0027	-0.0525
F	34.80	-0.0412	0.0035	-0.0485
G	45.80	-0.0119	0.0014	-0.0292

μ_{δ} = mean
 σ_{δ} = standard deviation

Generally, the model predicted the data within one standard deviation. The only exception occurred at the north end of the bridge, where the prediction was nearly 50 percent greater than the actual deflection. This, the quarter-point truck location, was, however, close to the triangular steel gusset plate. Given such small deflections, it is possible that the plate was providing more strength in that corner of the bridge than the model, which simulated the plate with five vertical, fixed-connection members, predicted.

The following calculations compare the overall stiffness of Morgan Bridge, first as calculated using the computational model results, and then using the field results. For these calculations, it was assumed that the overall stiffness was equal to the mid-span stiffness with the live load at location D.

$$k_{model} = \frac{4300 \text{ kips}}{0.0525 \text{ in.}} = 81,900 \text{ k/in.}$$

versus

$$\frac{4300 \text{ kips}}{(0.0499 + 0.0027) \text{ in.}} \leq k_{experimental} \leq \frac{4300 \text{ kips}}{(0.0499 - 0.0027) \text{ in.}}$$

$$81,750 \text{ k/in.} \leq k_{experimental} \leq 91,100 \text{ k/in.}$$

The predicted stiffness was within the possible range of stiffness determined from field measurements (considering instrument error). Given the practical assumptions needed for the model, this was good agreement.

Lower Chord Scarf Joint Behavior

Scarf joints have been used in many timber bridges as a solution to the problem of

transferring tension forces across a connection between two pieces of wood. The Morgan Bridge is no exception, and it employs three scarf joints on each bottom chord to “splice” together two pieces of wood. The bottom chord appears to be part of the original structure, as evidenced by the scarf joints that are worn down and cracked from years of use. The following diagram illustrates how scarf joints would have originally worked.



Figure 25. Scarf joint mechanism

Field tests were performed using an extensometer in an attempt to determine the extent to which the scarf joints were still functioning. The scarf joints in both the interior lower chord member near the quarter point and the exterior lower chord member at mid-span were tested. The extensometer was positioned to span the top of the joint. Figure 26 is an illustration of the lower chord, showing the positions of the scarf joints. Three trials were performed for each joint location, and for each trial data was recorded with the truck at six different positions along the span: A, B, C, D, F and G (see Figure 8).

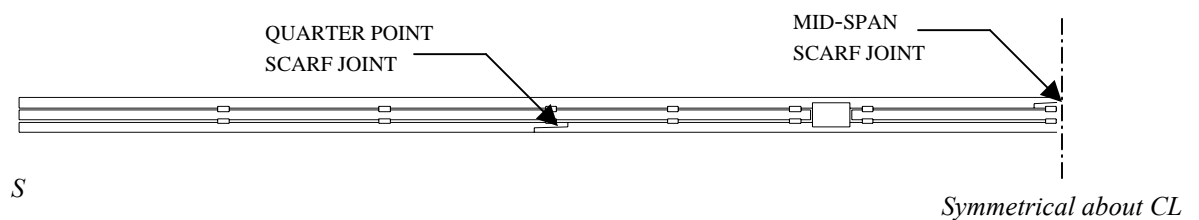


Figure 26. Plan view of southern half of lower chord showing locations of scarf joints

Figures 27 and 28 show the extensometers in place at the two scarf joints.

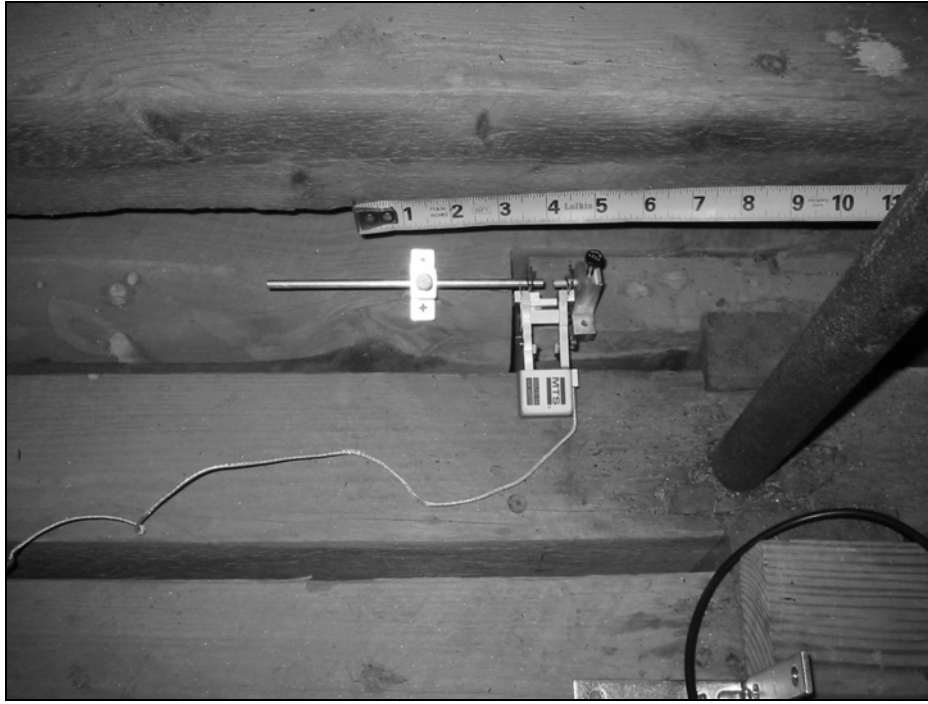


Figure 27. Extensometer spanning the scarf joint at mid-span

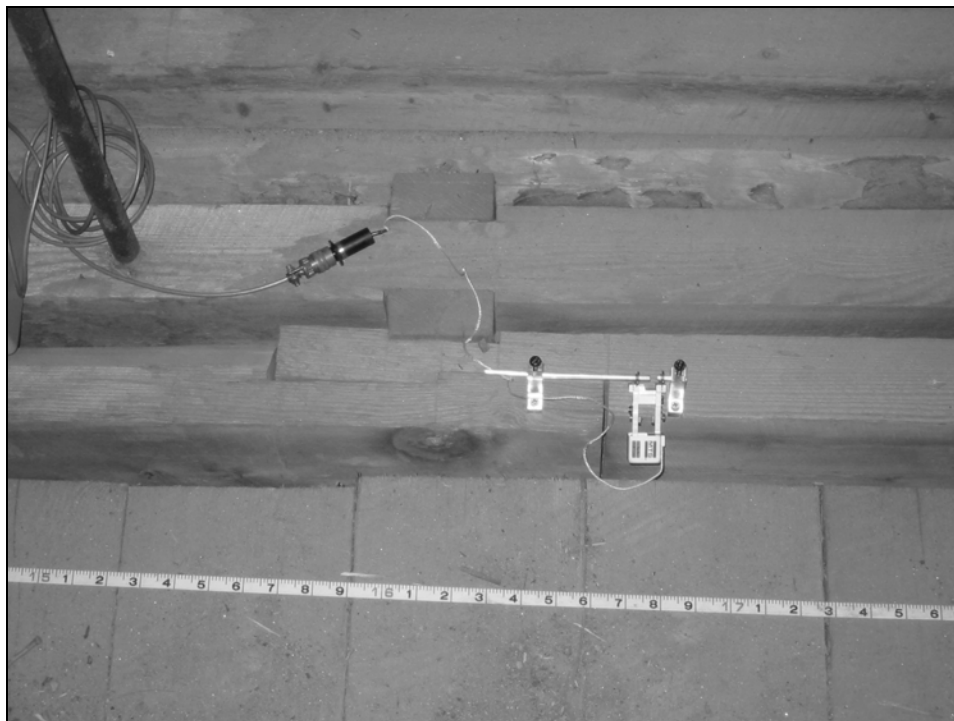


Figure 28. Extensometer spanning the scarf joint at quarter point

Results of the data collected from the extensometer are provided in Figures 29 and 30. For both plots, the independent axis demonstrates the location of the vehicle's center of gravity along the west truss, with zero at the south end. The movement of the scarf joint is shown on the dependent axis.

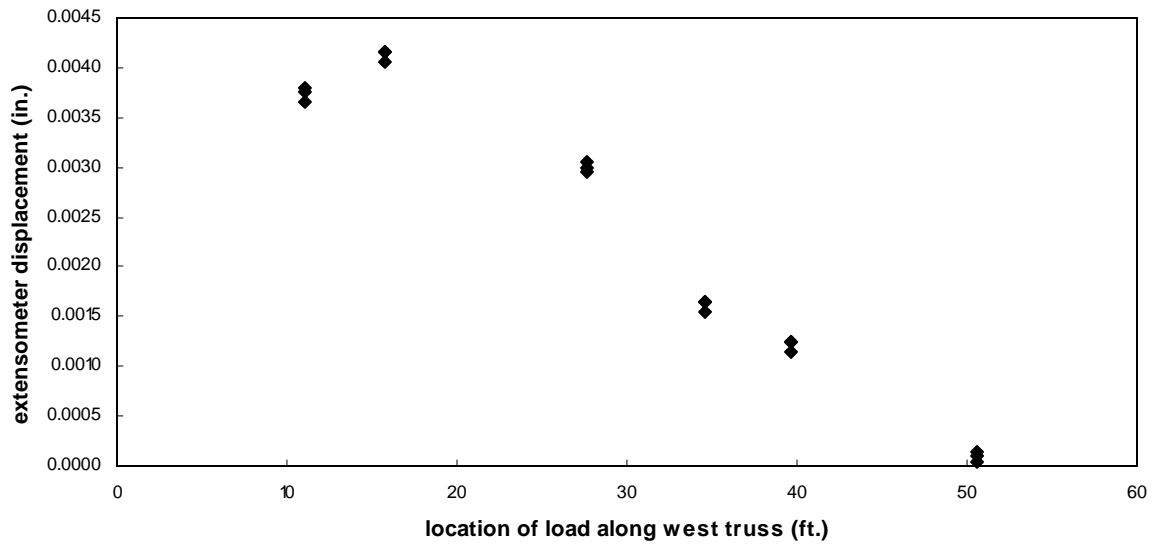


Figure 29. Results of extensometer placed at the mid-span scarf joint

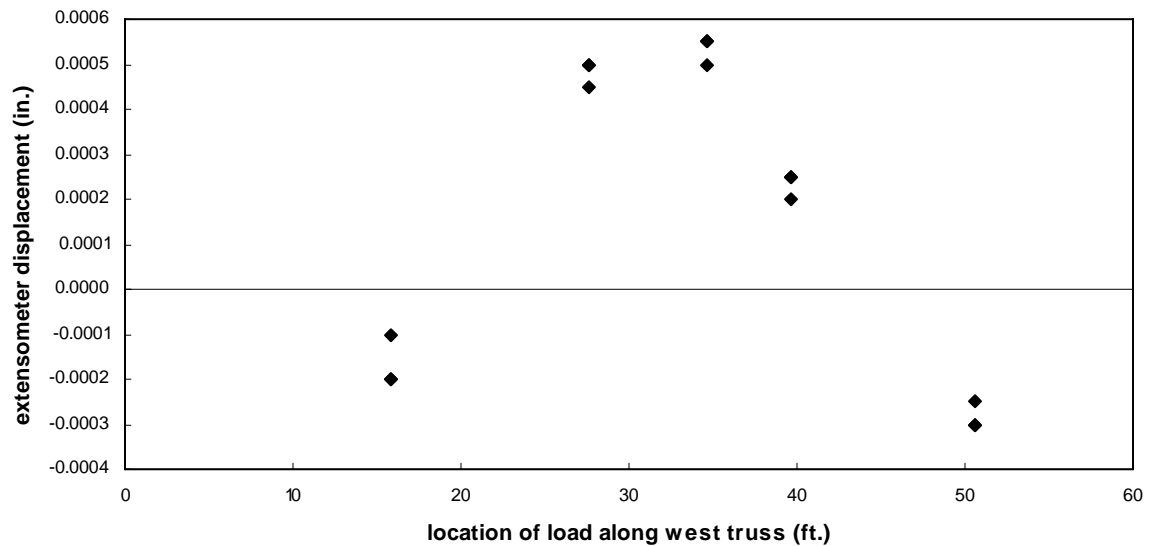


Figure 30. Results of extensometer placed at the quarter-point scarf joint

Initially, it was thought that the scarf joint would act as a “pointer,” such that a positive result would indicate the two members were pointing upward (\wedge) and a negative result would indicate that they were pointing downward (\vee). According to the influence line in Figure 29, however, this would mean that the mid-span scarf joint consistently pointed up, even though the deflected shape at mid-span suggested just the opposite. Rather, it seems the results indicate that the scarf joint was not rotating at all, but was simply opening up as a result of tension in the bottom chord. Still, it is not clear why the mid-span joint would open more with the truck near the south end than it did with the truck near the north end. Nor is it clear why the scarf joint at the quarter point closed with the truck near either end of the bridge, since the bottom chord was always in tension, regardless of the truck’s position.

One thing is clear from the findings—the assumption in the model that the areas around scarf joints did not contribute to the strength of the bottom chord was justified. If a stronger correlation between magnitudes of force in the bottom chord and the magnitude or direction of scarf joint movements existed, it would have been plausible to assume that some force was being transferred through that connection. For instance, if the mid-span scarf joint had opened its maximum amount with the truck at mid-span and less with the truck near the ends, it might well have indicated that the two sides of the spliced bottom chord member were reacting to the increased force in the chord, engaging more as the tension force increased and less as it decreased. As the results show, there was no such correlation to suggest that the movements are in any way related to the magnitudes of the tension forces.

Wood Joint Behavior

For covered wooden bridge builders, one of the main design goals was to minimize the number of tension connections. Unlike compression joints, wooden joints that functioned efficiently and reliably in tension were difficult to fabricate and maintain. This goal was apparent from the two earliest truss designs, the kingpost and queenpost. As discussed above, tension connections occur only where the vertical posts meet the top and bottom chords, and between adjacent bottom chord members. In the Morgan Bridge, the bottoms of the queen posts were notched to transfer tension force in the form of bearing pressure to the bottom chord, while mortise-and-tenon joints were employed for the same purpose at the tops of the posts. Where adjacent timbers were needed to make up the length of the bottom chord, the scarf joints just discussed were used. These joints also transfer tension by way of bearing pressure between the interlocking knuckles.

If the application of live load causes a member in compression under dead load to see tension instead, its compression joints cannot transfer this tensile load to the rest of the bridge, rendering the member useless. For early bridges—those built before prestressing became common—the usual way to avoid this kind of stress reversal was to

be sure the compression force from the dead load was great enough to maintain a net compressive force, even when live loads tended to reduce it. Thus, the joints would remain tight. This was the case for the original configuration of Morgan Bridge.

When Morgan Bridge was rehabilitated in 1979, two counterbracing timber members were added to the center panel. While apparently installed to give better support to the center floor beam rods, their orientation is such that under dead load they are in compression. Interestingly, these members were toe-nailed in place, something that should not have been necessary in compression joints. (Exactly when this was done is not known.) When the live load was positioned with a significant portion within the exterior panels, however, the model predicted, and field testing confirmed, that these new counterbracing members experienced tension. Closer inspection of the structure revealed that one of these members has recently been replaced, possibly indicating excessive stress as it at some point.

This behavior is apparent in the axial force diagrams of Figure 31. The first two diagrams show the axial forces in the original bridge, first with live load alone (Figure 31a), then with the combined dead and live load (Figure 31b). The second two diagrams show the axial forces in the existing bridge, first with live load alone (Figure 31c), then with the combination of dead and live load (Figure 31d). The live load for all four diagrams in the model was placed at location A, where the maximum effect was observed in the field (see Figure 7). Note, however, that due to the difference in the number of floor beams between the original and existing bridges, the load distribution varied between the two models.

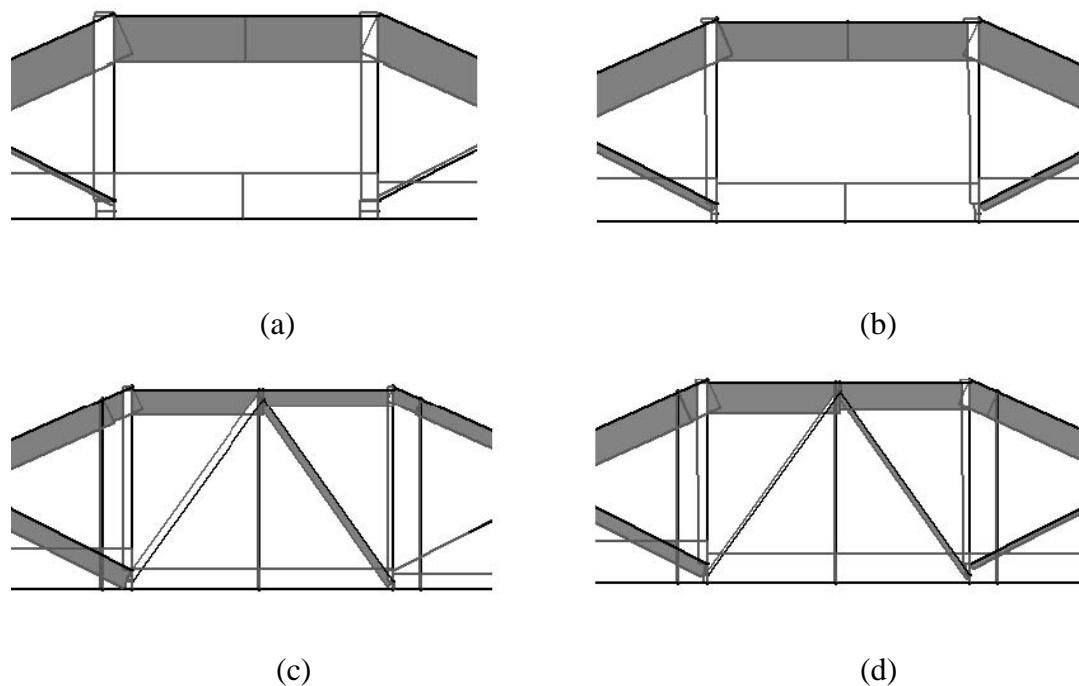


Figure 31. Axial force diagrams for (a) live load at A in original configuration, (b) dead and live load at A in original configuration, (c) live load at A in existing

configuration, and (d) dead and live load at A in existing configuration

Experimental field tests were performed to determine the validity of the computer model with respect to the existing configuration. With the difficulties of measuring strain in timber, it was decided instead to measure displacement across the joint between the south counterbrace in the center panel and the south queenpost. An extensometer was positioned along the longitudinal axis of the counterbrace, spanning its connection with the queenpost (see Figure 32). Three trials were performed, stopping the vehicle at five locations along the span each time to collect data.



Figure 32. Extensometer in place at the connection

The results of the field test and computational model are shown in Table 4 and Figure 33. Table 4 provides a comparison of the observed field data with the values predicted by the computer model. Figure 33 illustrates the data with the x-axis denoting the vehicle's location along the west truss (zero represents the south end), and the y-axis showing the amount of movement recorded in the joint along the longitudinal axis of the counterbracing member. A positive movement correlates to the joint opening up due to a net tensile force, while a negative movement correlates to its closing under net compression. The dashed line provides an approximate solution of the influence line for joint movement.

Table 4. Comparison of experimental results and predicted results for joint movement at queenpost – counterbrace connection

Truck Position		Field Data		Computer Model
Description	Location (ft)	μ_{δ} (in)	σ_{δ} (in)	δ (in)
A	11.05	0.0106	0.0006	0.0014
C	22.80	0.0005	0.0001	-0.0001
D	29.80	-0.0030	0.0001	-0.0020
F	34.80	-0.0038	0.0001	-0.0021
G	45.80	-0.0023	0.0000	-0.0010

μ_{δ} = mean

σ_{δ} = standard deviation

While the calculated and experimental magnitudes differ, their matching trends are clearly evident in Figure 33. The greatest variation between the experimental and computational results was when the live load was very close to the south abutment. The errors in the computed values were due to the model having a pinned joint at this location instead of one that suddenly became disconnected. In the field, the extensometer was observed to widen steadily as the truck moved past the queenpost location. It was apparent from both the experimental and computational analysis that the addition of these center panel diagonals added nothing to the performance of the truss system. In fact, the bridge is doing its best to remove them!

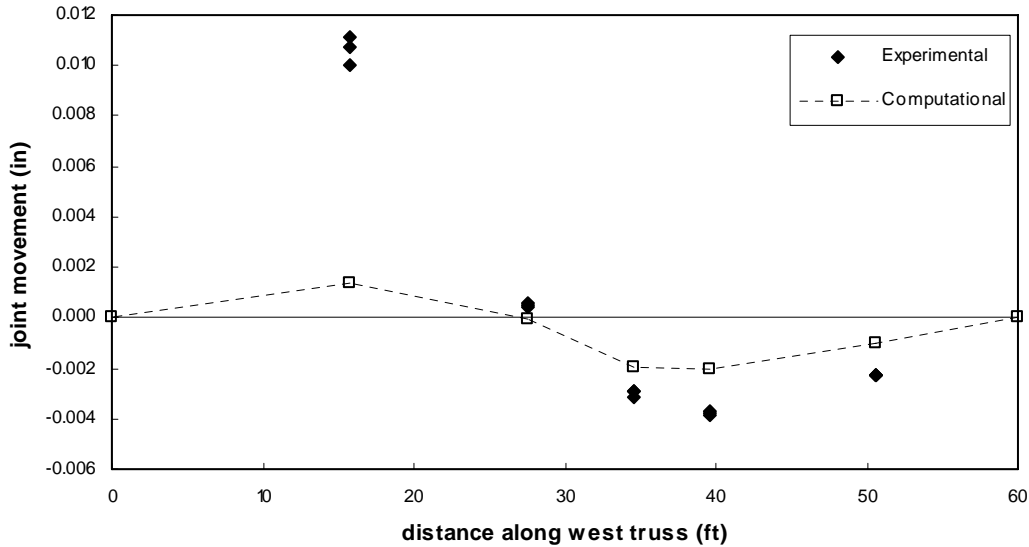


Figure 33. Comparison of influence lines for joint movement at queenpost – counterbrace connection

Influence of Metal Rods

Each truss (east and west) employs seven metal rods to convey vehicular live loads from the floor beams to the truss. Two of the rods are part of the original configuration, but the rest were added as part of the 1979 rehabilitation. Without definitive information, it has been assumed throughout this study that all of these rods were made from steel. In the field, strain gages were mounted to three of them to get a better understanding of the loads they carried. The locations of the instrumented rods are illustrated in Figure 34.

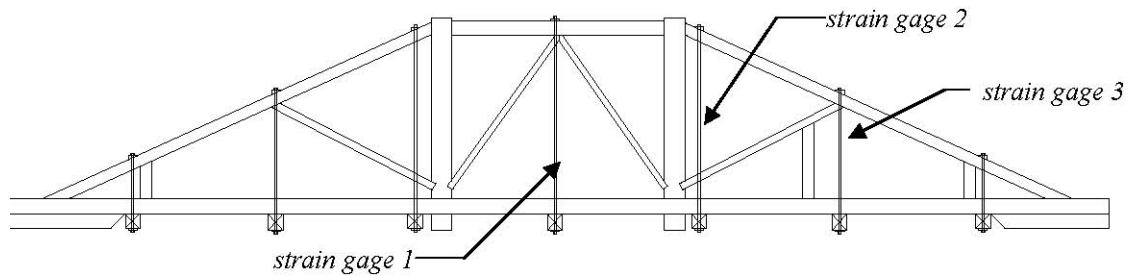


Figure 34. Strain Gage Locations along West Truss

Twelve trials were performed for each rod: three with the truck at location C, six at D, and three at location G (see Figure 7). The results of the data collected from the strain gages are shown in Table 5. A positive strain indicates axial tension, and a

negative strain indicates compression. Strain gage data was read in microstrains from a strain indicator unit that was connected to all three strain gages.

To test the predictions of the computational model, the strains were computed using the initial and final lengths of the corresponding metal rod elements and the following equation. These results are also shown in Table 5.

$$\epsilon_{rod} = \frac{L_{final} - L_{original}}{L_{original}} = \frac{\Delta L}{L_{original}}$$

Table 5 Comparison of experimental and computation results for strain in metal rods

Member	Truck Position		Field Data		Computer Model
	Description	Location (ft)	μ_{ϵ} (in)	σ_{ϵ} (in)	ϵ (in)
Rod 1	C	27.6	27.6667	1.1547	21.3135
	D	34.6	20.8333	3.2506	22.2804
	G	50.6	-9.6667	1.5275	0.6946
Rod 2	C	27.6	7.3333	1.5275	5.8743
	D	34.6	22.0000	9.0111	13.2619
	G	50.6	1.3333	1.5275	-1.0333
Rod 3	C	27.6	1.0000	0.0000	-0.6908
	D	34.6	7.8333	0.7528	-0.4979
	G	50.6	39.0000	0.0000	53.0203

μ_{ϵ} = mean

σ_{ϵ} = standard deviation

In addition to the Table 5, Figures 35, 36, and 37 show the position of the model prediction within the range of experimental data for each rod. Considering the sensitivity of strain gage instrumentation, the results are reasonable. For the most part, the model predicted values that followed the general trend of the strains, even if the predictions were outside the range of error.

It is interesting to note the number of times a negative value crept into the results, which indicated a rod was being compressed. It was surely not the intention of either the original builders or the engineers who designed the rehabilitation for this to happen, but while the magnitudes differ, both the experimental and computational results predict such behavior. Of course the computational results could be affected by limitations on connection modeling, but in the field, the rods should be free to slide up and down through their connections to the truss members. Since the instrumentation picked up compression, the connections must be preventing this free movement.

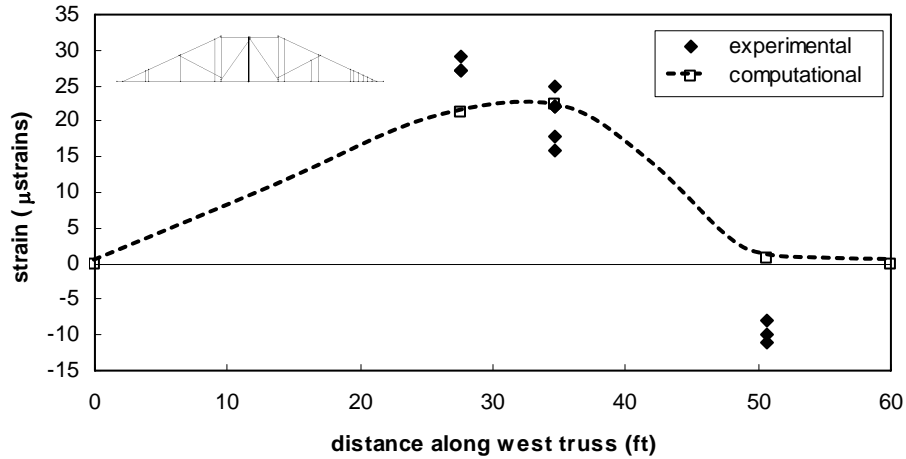


Figure 35. Influence line for strains in Rod 1

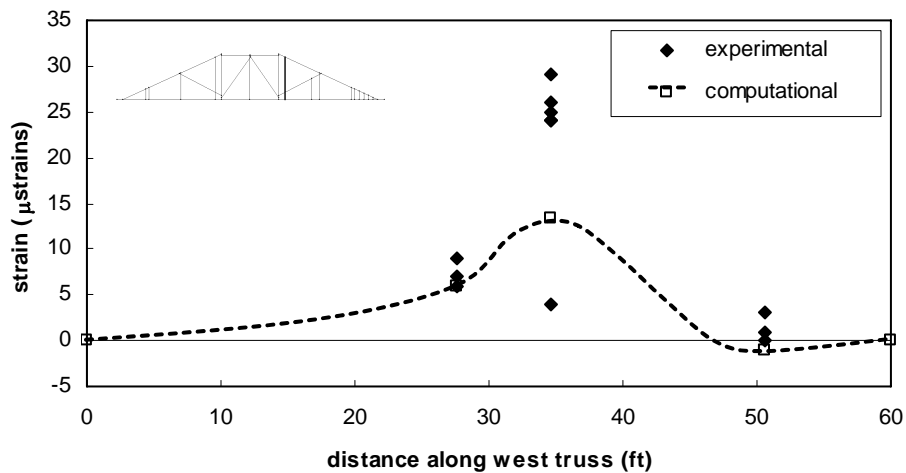


Figure 36. Influence line for strains in Rod 2

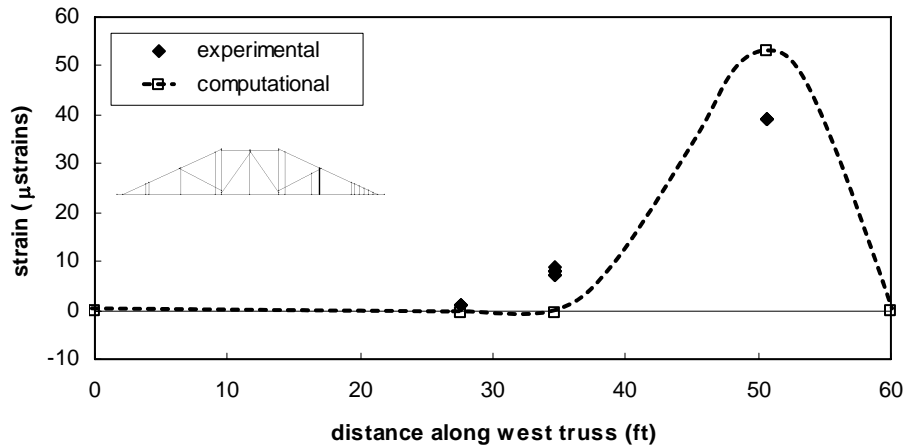


Figure 37. Influence line for strains in Rod 3

The variations between experimental and computational data are interesting; since the model overestimated how much load a particular rod was carrying in some instances, but underestimated it in others. In particular, the model underestimated the load sharing of Rod 2, and overestimated the load sharing of Rod 3. In the case of Rod 3, it is likely that a more significant portion of the load was transferred back to the abutment by way of the stringers and bolster beams than the model predicted, as this is a well-documented occurrence in truss bridges.

A greater concern was the gross underestimation of the load carried by Rod 2. Rod 2 was added in 1979 along with the addition of a floor beam adjacent to the queenpost. While it was most likely intended for the rod to transfer load to the bottom and top chords, thence to the queenpost, two possibilities seem likely. Either the queenpost was no longer capable of carrying a majority of the load, or the chords were no longer transferring this load to the queenpost, thus requiring the rod to carry a significantly larger force.

Panel Shear

The role of the web in a steel beam is much like the role of the vertical and diagonal members between two chords of a truss. That is, they are both a means of transferring shear forces and maintaining stability in the beam or truss. Depending on the orientation of the diagonal, shear forces in a truss may be transferred through tension or compression. A simple example to describe this mechanism is a square box, shown in Figure 38a. When subjected to shear forces, the box will tend to deform as shown in (b). To resist this deformation, diagonal members may be added as shown in (c) or (d). The orientation of the diagonal member does not affect the magnitude of the force that it resists, but it does determine whether the method of resistance is tension or compression.

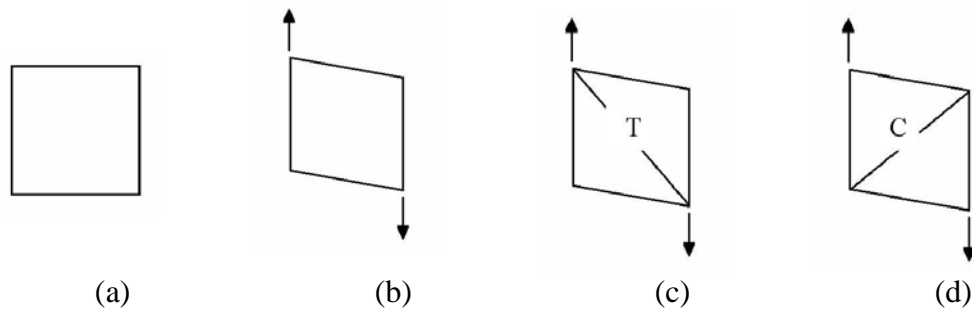


Figure 38. Shear force in a square truss panel

A queenpost truss like the Morgan Bridge has such a square center panel, and diagonals were added to it in the 1979 rehabilitation. To investigate the distribution of shear forces in this panel, two position transducers were arranged as shown in Figure 39. This location was chosen based on preliminary computational model results predicting the maximum deflection to be in this panel. Figure 40 shows the influence line for panel shear developed from the field test data.

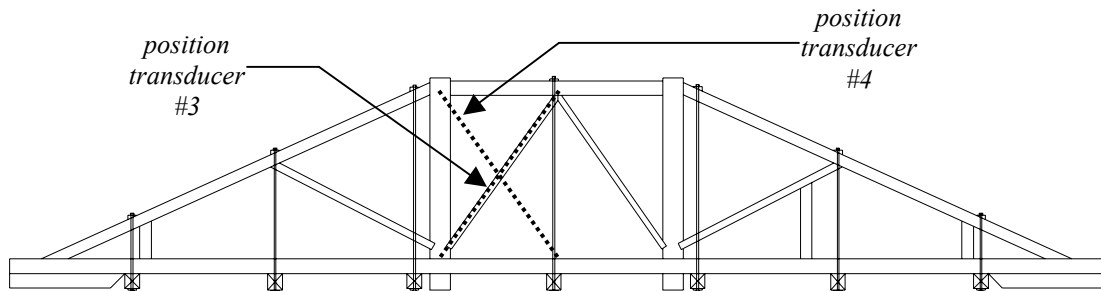


Figure 39. Location of Position Transducers on the West Truss

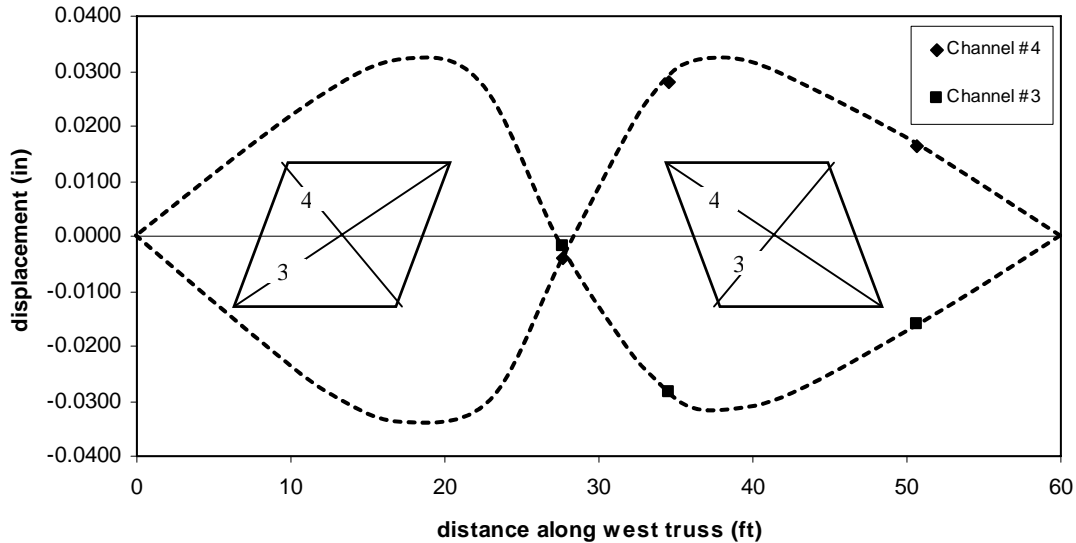


Figure 40. Influence line for panel shear

As in the previous graphs, the x-axis indicates the location of the vehicle's center of gravity along the west truss, with zero at the south end. The y-axis denotes the expansion and contraction between the ends of the two position transducer cables. A positive mean displacement correlates to an expansion along the line of the transducer, and a negative mean displacement correlates to a contraction. Since the bridge was primarily loaded on its northern half for this test, position transducer 4 consistently contracted from its unloaded position and position transducer 3 consistently expanded. At the position closest to the south abutment (0 feet), the results of the transducers are just beginning to cross each other. Had the experiment been carried out closer to the south abutment, it is likely that position transducer 4 would have expanded and position transducer 3 contracted, as shown by the proposed influence line in Figure 41.

Initial comparisons of the model to the experimental results indicated that the model was too stiff with regard to panel shear deformations. The “computational – with diagonals” line in Figures 44 and 45 describes these results. It was determined that there were two possible reasons for this error in model prediction. The first is that the queenpost, to which one end of both position transducers were attached, was sharing more of the load with the adjacent steel rod than predicted. This was previously suggested as a reason for discrepancies in model prediction of strain gage results related to this rod. Another possibility is that the counterbracing diagonals in the center panel were not accurately modeled due to their cyclical loading. With different structural analysis software, it might have been possible to describe these members as gap elements (members released under tension forces), as that is what happens in a system such as this. To illustrate an “upper-bound” of the computational data in Figures 41 and 42, the deformations with both counterbracing members removed is shown with the other data.

These results demonstrate that the actual effectiveness of the bridge in transferring shear forces is somewhere between these two extremes.

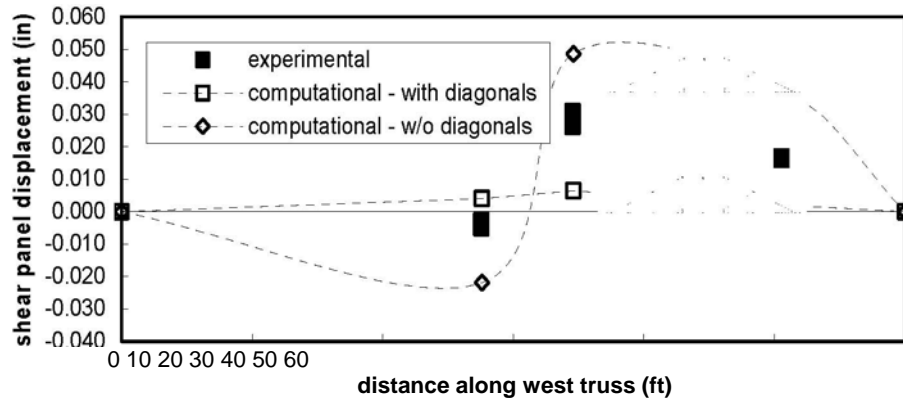


Figure 41. Influence line for panel shear displacement predicted compared with experimental statistical data (Position Transducer 4)

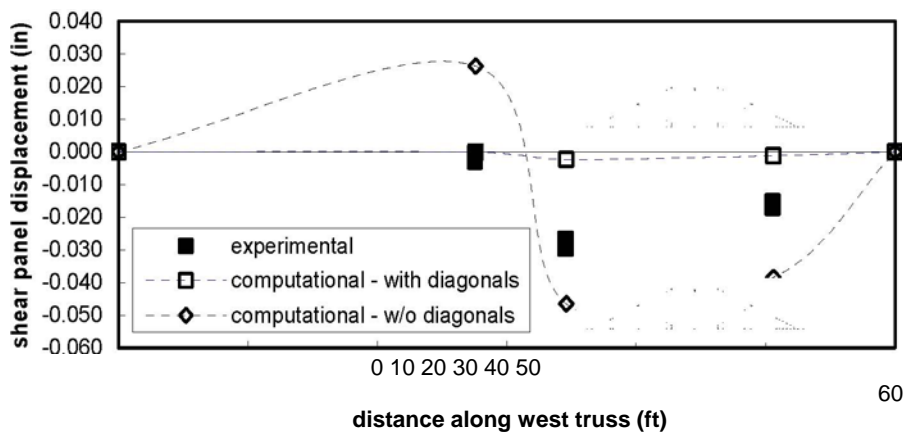


Figure 42. Influence line for panel shear displacement predicted compared with experimental statistical data (Position Transducer 3)

Three-Dimensional Behavior under Live Load

In general, truss bridges are analyzed as two-dimensional structures, with the assumptions that there are no significant eccentricities in either the structure or the loads, and that the trusses are adequately braced against lateral forces. For the Morgan Bridge, differences between the east and west trusses, such as the triangular gussets in two corners, make the occurrence of significant eccentricities a realistic possibility. To investigate this, two position transducers and an LVDT were connected between the east and west trusses to measure relative out-of-plane displacements under vehicular loading. The locations of the instruments are illustrated in Figure 43. Figure 44 is a photograph of

the assembly.

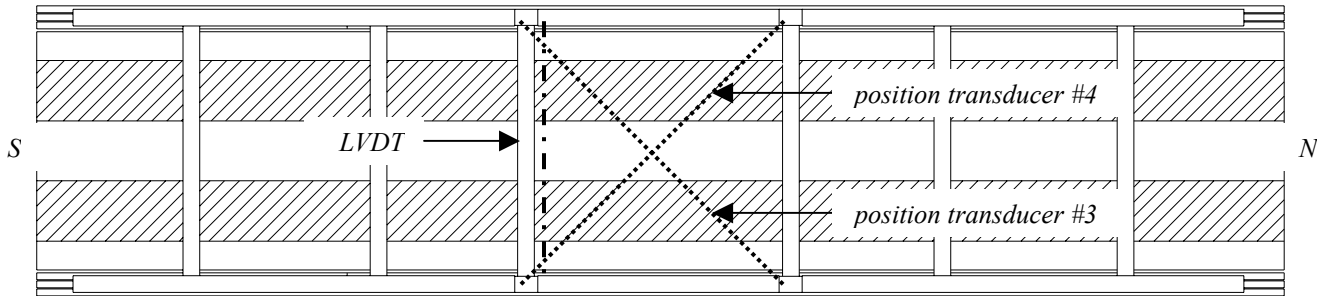


Figure 43. Plan view of bridge, showing locations of the position transducers and LVDT



Figure 44. Photograph of test assembly (looking south)

Tests were performed with the truck at positions C and G, although there were no out of plane movements detected with the truck at G, so only C will be discussed here (see Figure 7). It is likely that position C provided the most significant results because it placed the truck in the same panel as the instrumentation. In fact, the axle positions are

nearly symmetrical about the mid-span of the bridge. Three trials were performed, with significant variation among results. Both the mean and standard deviation are reported in Table 6.

Table 6. Comparison between experimental and computational out-of-plane displacements

Cable Location	Field Data		Computer Model
	μ_{δ} (in.)	σ_{δ} (in.)	δ (in.)
A - D	-0.0009333	0.001617	-0.00000065
A - C	0.003192	0.001689	-0.00098
B - D	-0.001490	0.002052	-0.0022

μ_{δ} = mean

σ_{δ} = standard deviation

To evaluate the experimental results, a three-dimensional computer model was developed, based on the two-dimensional model, but with the addition of floor beams and roof truss members. Field measurements were not made of the east truss, but a triangular steel plate was observed at its south end, identical to the one at the north end of the west truss. Assuming that this would be the most significant contributing factor to the results of the model, the east truss was modeled as a 180-degree rotation of the west truss about the vertical axis. The transverse members of the roof truss were included in the three-dimensional model. To account for the apparent stiffness of the knee braces, the joints between the roof members and the trusses were assumed to be fixed. The floor beam connections to the trusses were modeled as pins, assuming that no moment could be transferred through the metal rod connection. The three-dimensional model is shown in Figure 45.

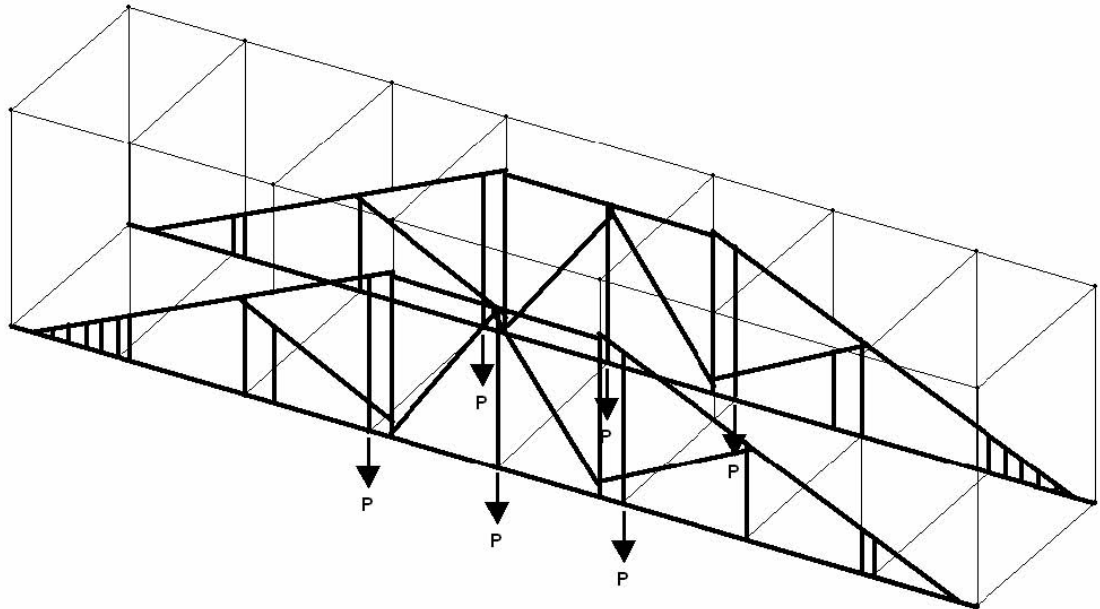


Figure 45. Three-dimensional MASTAN model of Morgan Bridge with truss loading shown for truck at position C

The model was loaded just as for the two-dimensional model, with the appropriate concentrated forces applied to the panel points. Since the floor beams were pin-connected to the truss, loading the truss anywhere along the floor beam would be suitable, since no moment from the floor beam could be transferred to the truss. Figure 46 illustrates the undeflected shape of the roof truss (as viewed from above) and the deflected shape of the roof truss when loaded at position C. The darkened lines represent the LVDT and position transducer locations. Table 6 contains the results of both the experimental tests and the computational model.

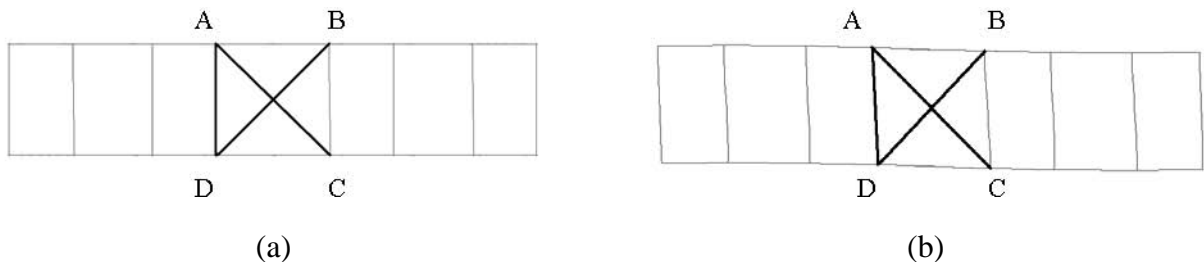


Figure 46. (a) Undeflected and (b) Deflected shape of roof truss with live load at position C

While the two sets of results are not at all close to the same magnitude, they do both represent a similar type of deformation at the top of the truss. As the deflected shape in Figure 46(b) shows, the position transducer connecting points A to C should be in tension, or positive, while the position transducer connecting points B to D should be in compression, or negative. This was demonstrated nicely by the experimental results, but not quite as well by the model. Both results indicate that the transverse members in the roof truss were compressed, which is somewhat intuitive since the live load was applied to the floor.

While neither method (experimental or computational) resulted in large displacements—in fact, they were quite small—the experimental displacements were significantly higher in magnitude than the model predicted.

Live Load Survey

Part of the experimental testing included surveys of the bridge before and after the application of live load to get an image of its overall deflection. The reflective prism targets were positioned in two ways. The first was done to yield the deflection at the top of each panel point, and the second to compare relative deflections between the east and west trusses. The results of the first test are illustrated in Figure 47, which shows a comparison of deflected shapes between the computer model loaded at mid-span, and the computer model with settlements equal to measured deflections.

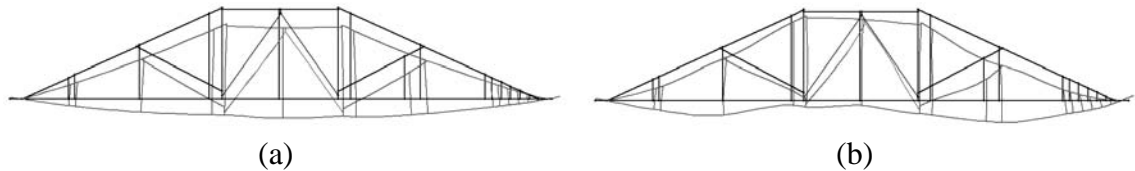


Figure 47. Deflected shapes with live load at E as indicated by (a) computer model and (b) field survey

There were clearly errors in the deflections obtained, as evidenced by the above figure. This was not surprising due to a number of factors, not the least of which was human error. The survey equipment required the operator to line up the prism, as viewed through a lens, with cross hairs in the total station. The process was tedious, and since the deflections were occurring only in the vicinity of the highest possible tolerance (1 mm = 0.03937 in), they could easily have been affected by the slightest human error. Accordingly, this experience indicated that surveying is not a useful tool for this type of experiment, especially when the expected deflections are within the range of equipment tolerance.

CONCLUSIONS

This analysis of the Morgan Bridge demonstrated that the combination of experimental load testing and computational modeling is of significant value in the structural analysis of a timber structure. This combination provided an understanding of the behavior of a unique, nineteenth-century timber structure that could not have been gained with the use of either method alone. Considerable insight was gained into the bridge's behavior, both as it exists today, and as it may have looked 100 years ago. Insight was also gained into what works and what does not in a computational model of a timber structure.

In general, the computational and experimental results were in good agreement, which was encouraging since bridge design engineers in the United States do not extensively use experimental load testing. The only significant difference between the experimental evidence and computational model prediction was in the shear panel deformation test. Further testing of the counterbracing members in the center panel, as well as the queenpost, would be required to fully understand the disparity.

Other definitive results of the analyses indicated that the rehabilitation work done in 1979 did not appreciably change the load-carrying behavior of the main trusses, but it did introduce members, the center panel diagonals, that are unlikely to ever perform well due to cyclical forces in their connections under typical live loading. Even with some of the unusual and asymmetrical detailing done during the rehabilitation, the system remarkably displays little out-of-plane displacement.

The most noticeable contribution of the rehabilitation, though difficult to accurately model, was the stiffening of the floor system and subsequent alteration of live load distribution. With only three floor beams, as opposed to the seven that exist today, it is likely that a more significant portion of the load was at one time carried through the floor system to the abutments. The load-sharing role of the hanger rods, along with the additional floor beams, was not accurately determined, but there was some indication that they are more active in carrying the load than the simplified computational model might suggest. Finally, in comparing the computational model with a series of load tests performed on the scarf joints, it was determined that they are no longer effective at transferring axial forces between lower chord members.